Kinetic features of the chemiluminescent oxidation of *N*-octylluminol by the hypochlorite ion in a self-organized micellar medium

T. V. Yan′kova,[a,b] P. V. Mel′nikov,[a]★ V. R. Flid,[a] and N. K. Zaitsev[a]

[a]*MIREA — Russian Technological University (M. V. Lomonosov Institute of Fine Chemical Technologies), 86 prosp. Vernadskogo, 119571 Moscow, Russian Federation*
[b]*Research Technical Center of Radiation Chemical Safety and Hygiene, Federal Medical Biological Agency, 40 ul. Shchukinskaya, 123182 Moscow, Russian Federation.*
E-mail: melnikovsoft@mail.ru

For the model chemiluminescent reaction of *N*-octylluminol, a hydrophobic analogue of luminol and a surfactant, a scheme was established and parameters of the formal kinetic equation were calculated. The formation of intrinsic micelles of the substrate promotes a triple increaese in the rate of the first step of the luminogenous reaction and a multiple increase in the detected maximum and integrated signal intensities compared to results obtained in the classical chemiluminescent system based on luminol.The reversible conversion of *N*-octylluminol to a non-luminescent form was revealed, and the equilibrium is strongly shifted to the latter, which distorts the shape of the detected kinetic curve and decreases the analytical signal with time. This shift can be prevented by using the systems with controlled mixing of reagents.

Key words: chemiluminescence, micellar systems, luminol, luminol analogue, reaction mechanism, reversible reactions.

Chemiluminescent reactions are presently used widely for the solution of various analytical problems in both monitoring of the environmental state and medicine.[1,2] Chemiluminescent immunoassay is characterized by a broad linear range and a low noise background, and moderate prices of the relevant equipment. At the same time, the step of the intrinsic chemiluminescent reaction is not selective.[3] The method is also applied for the determination of the spatial distribution of reactive oxygen species.[4,5] Another important application of chemiluminescence methods is the determination of the total viable count (TVC) based on the reaction with adenosine triphosphate (ATP), which is present in bacterial cells and transforms into adenosine monophosphate (AMP). Two chemiluminescent systems based on the enzymatic oxidation of luciferin and chemical oxidation of luminol were developed for the determination of the TVC. In the first system, ATP initiates the bioluminescence of luciferase, and the chemiluminescence intensity depends linearly on the amount of ATP, which transforms into AMP and pyrophosphate (PP)[6,7] (Scheme 1).

Scheme 1

$$\text{D-Luciferin} + \text{ATP} + O_2 \xrightarrow{\text{Luciferase, } Mg^{2+}} \text{Oxyluciferin} + \text{AMP} + \text{PP} + CO_2 + h\nu$$

To stabilize ATP, it is extracted with benzalkonium chloride (BAC),[8] but the latter inhibits luciferase decreasing the efficiency of bioluminescence. The introduction of liposomes into an analytical system makes it possible to bind BAC thereby preventing the inhibition of the chemiluminescent reaction and lowering the detection limits by an order of magnitude. Although this system has undisputable advantages, a substantial inherent drawback is its thermal lability often leading to a significant distortion of results upon improper storage or service.

When the TVC is determined by the reaction of luminol with hydrogen peroxide, ATP initiates the luminol chemiluminescence, the intensity of which is directly proportional to the ATP concentration.[9] The reaction proceeds *via* Scheme 2.

Scheme 2

$$\text{Luminol} + H_2O_2 + \text{ATP} \longrightarrow \text{3-Aminophthalate} + N_2 + H_2O + \text{AMP} + \text{PP} + h\nu$$

An important feature of the reaction is that the type of microorganisms can be determined from the shape of the detected kinetic curve,[10] since the time of achieving the maximum chemiluminescence intensity increases in the order fungi → yeast → bacteria. The observed kinetic

Published in Russian in *Izvestiya Akademii Nauk. Seriya Khimicheskaya,* No. 12, pp. 2294—2301, December, 2020.
1066-5285/20/6912-2294

changes are associated with the morphology and specific features of biochemical systems of cells with different structures. Unlike luciferase, luminol is much more stable and can be stored in the dry form for years, but the system has a substantial drawback: significant inaccuracy and high detection threshold, which enable only qualitative determinations. However, various approaches are used to overcome this drawback, for example, the application of micellar media.[11] Owing to the microconcentration effect and separation of the substrate and intermediate products, these approaches can give an additional possibility to study the mechanism of chemiluminescent reactions. Using these approaches, one also can increase sensitivity and extend the range of analyzed objects, for instance, by decreasing the influence of the analytical matrix or combining components with limited mutual solubility.[11]

Thus, the threshold of determination of L-thyroxine can be decreased to $8.9 \cdot 10^{-9}$ mol L^{-1} by the introduction of cetyltrimethylammonium bromide (CTAB) into a luminol—potassium permanganate chemiluminescent system, and the linear range is $5.0 \cdot 10^{-8}$—$3.0 \cdot 10^{-6}$ mol L^{-1} in this case.[12]

It is shown for a luminol—hydrogen peroxide chemiluminescent system and a number of surfactants (CTAB, cetylpyridinium bromide, sodium dodecyl sulfate, dodecyl polyoxyethylene ester) that the chemiluminescence intensity increases with an increase in the surfactant concentration but decreases significantly after passing through the CMC point.[13]

The chemiluminescence intensity caused by the effect of the local concentration increases significantly due to the addition of fluorescent acceptors to a system of luminol and its analogues. This enhances the intramicellar energy transfer even for substances with a very low quantum yield ($\phi \geqslant 0.00001$).[14] The plasmon resonance appears in the presence of metallic nanoparticles, which also results in a significant increase in the intensity of the detected signal,[15] but the analysis becomes considerably more expensive.

It has previously been shown that luminol in a micellar solution is localized in the aqueous phase.[16] To remove the chemiluminescent substrate in the micellar phase and to use the effect of the local concentration, we developed a procedure for the synthesis of its hydrophobic analogue: *N*-octylluminol.[17] Owing to the long hydrocarbon radical and negatively charged center (in an alkaline medium), this molecule can form intrinsic micelles. The addition of a nonionogenic surfactant to a chemiluminescence system of *N*-octylluminol results in an increase in the chemiluminescence intensity.[18]

Since the transition to heterophase systems enhances the possibility of changing the mechanism of interaction of the components, it was desirable to reveal the specific features of kinetics of the chemiluminescent oxidation of *N*-octylluminol by the hypochlorite ion in a self-organized micellar medium. This system is a convenient model, because the hypochlorite ion is more stable than ATP. A chemiluminescent system with the same set of components but in the presence of a classical luminogenous substrate luminol was used as a reference.

Experimental

N-Octylluminol ($C_{16}H_{23}N_3O_2$) was synthesized according to a described procedure.[17] Luminol ($C_8H_7N_3O_2$, 98.8%, Applichem, USA), sodium hydroxide NaOH (reagent grade, LenReaktiv, Russia), hydrogen peroxide (42.5%, MosKhimTorg, Russia), and hypochloran-3 (NaClO, 3.25%, NKF Omega-Dent, Russia) were used as received. Deionized water was prepared by passing water through the Aqualab AL Double water treatment system (Mediana-Filter, Russia). The quality of water was monitored by an Expert-002 conductometer (Econix-Expert, Russia) with a bulk-type sensor. The specific electric conductivity of deionized water was 1 μS cm^{-1}.

An experimental sample of a chemiluminometer (Econix-Expert, Russia) with four sensors (silicone solid photoelectron multipliers) operating in the mode of counting the number of quanta and arranged in different positions relative to a measuring cell (transparent glass tube) was used for the detection of chemiluminescence. The readings of the sensors were summated.

A solution of hypochlorite (0.25 mL) with a concentration of $4 \cdot 10^{-4}$ mol L^{-1} was placed into measuring cell and stored until the background light intensity not exceeding 100 quantum s^{-1} was established.[17] An alkaline solution of the substrate containing the luminogenous substance ($1.5 \cdot 10^{-3}$ mol L^{-1}) and sodium hydroxide (0.1 mol L^{-1}) was prepared. This alkaline solution was kept in a special vessel and at certain time intervals (t_{mix}) was introduced into a hypochlorite solution with a syringe needle through a rubber membrane. The result of measurements was detected as a kinetic curve of chemiluminescence in the coordinates intensity (arb. units)—time with a resolution of 0.2 s.[17] The maximum intensity (I_{max}) was determined from the peak height on the kinetic curve of chemiluminescence, and the total intensity (I) was determined by integrating the obtained kinetic dependence.

A series of subsequent one-type measurements was carried out using the procedure described above with each measurement dependent on the time interval t_{mix} over which the freshly prepared alkaline substrate was stored before mixing with a hypochlorite solution. The evolution of the observed kinetic curves was then analyzed.

Results and Discussion

Although the mechanism operative in luminol oxidation in an alkaline medium by the hypochlorite ion was not established it is known[19] that the overall reaction proceeds via Scheme 3.

The chemiluminescence spectrum of luminol corresponds to the fluorescence spectrum of aminophthalic acid[20]; *i.e.*, step 3 (see Scheme 3) represents in fact the luminescence process of aminophthalic acid obtained in the excited state *in situ* in step 2. Therefore, step 3 occurs

Scheme 3

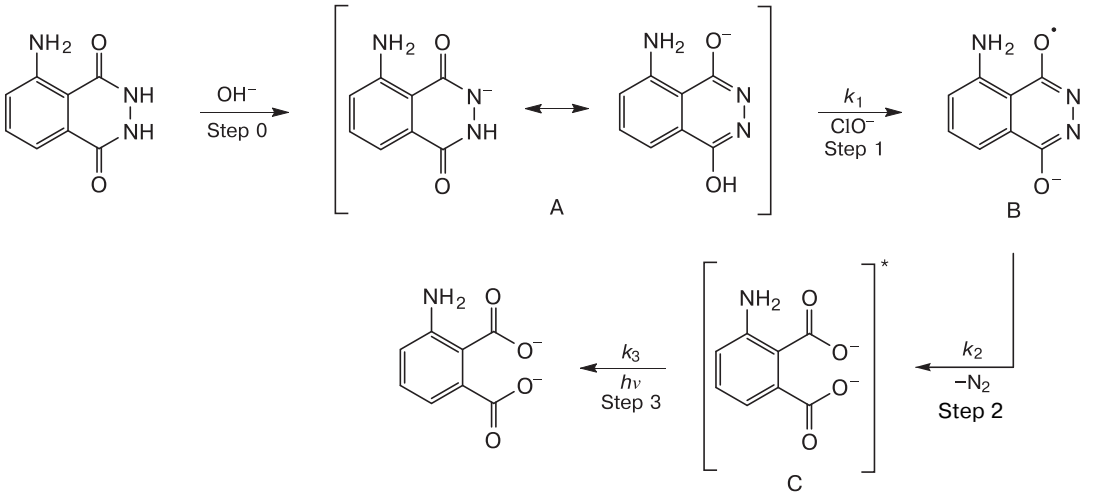

by several orders of magnitude more rapidly than other steps and the shape of the detected kinetic curves qualitatively corresponds to the formation and decay of the intermediate product in the consecutive reactions (Scheme 4).

Scheme 4

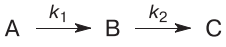

A is the active form of the luminol monoanion, B is the oxidized form of the luminol anion, and C is the excited molecule of aminophthalic acid.

Thus, the time dependence of the chemiluminescence intensity for luminol oxidation is described by a bell-shaped curve.[17]

For the reaction of *N*-octylluminol with the hypochlorite ion, the experimental time dependences of the chemiluminescence intensity (Fig. 1) differs from the kinetic dependence of luminol oxidation.[17] They resemble each other in shape at the first moment after reagent mixing (t_{mix}) and after 5 h (see Fig. 1, curves *1* and *10*, respectively). However, in this interval the distortion of the peak shape is observed first with an increase in the time from t_{mix} (see Fig. 1, curves *2* and *3*), and then the second

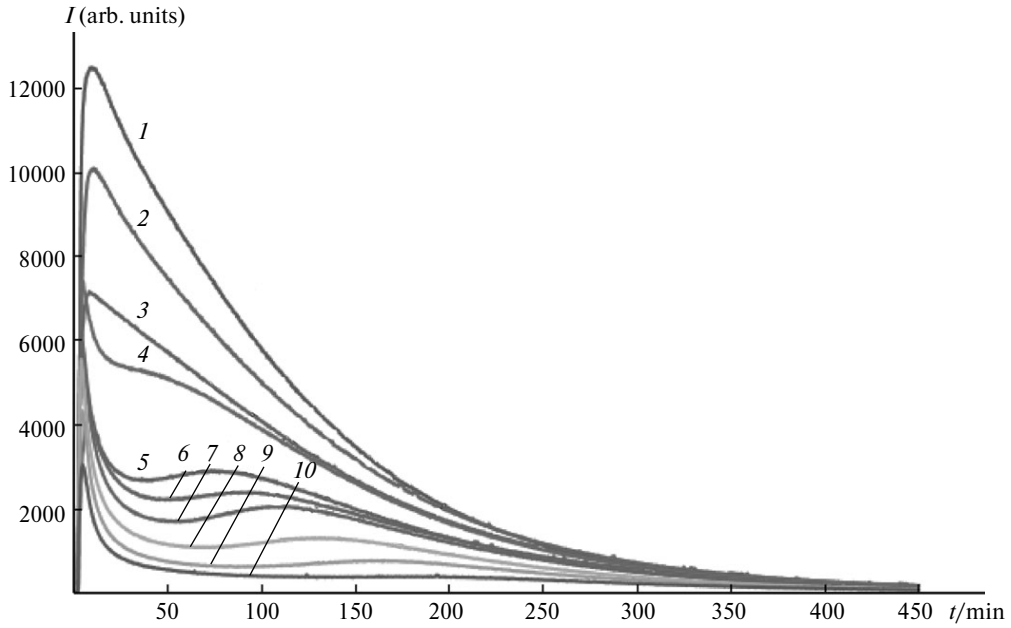

Fig. 1. Experimental kinetic curves of the chemiluminescent reaction of *N*-octylluminol ($1.5 \cdot 10^{-3}$ mol L^{-1}) with the hypochlorite ion ($4 \cdot 10^{-4}$ mol L^{-1}) registered after the time intervals (tmix) over which the freshly prepared alkaline substrate was stored before adding a solution of hypochlorite: 3 (*1*), 26 (*2*), 57 (*3*), 85 (*4*), 117 (*5*), 146 (*6*), 207 (*7*), 239 (*8*), 266 (*9*), and 296 min (*10*).

maximum appears on the kinetic curve (see Fig. 1, curves *4—9*), which then shifts gradually to the right (toward a longer time from the reaction onset), and later nearly disappears (see Fig. 1, curve *10*). During the transformation, the maximum intensity (I_{max}) shows a 3-fold decrease (see Fig. 1, curves *1* and *10*) and the total intensity (*I*) decreases 11 times.

Evidently, it is impossible to describe the observed evolution of the analytical signal for the oxidation of *N*-octylluminol by the hypochlorite ion in terms of Scheme 4. Two regions can conventionally be distinguished on the observed kinetic curve (Fig. 2). Region *1* (see Fig. 2) corresponds to the consumption of the current amount of substance A (*N*-octylluminol monoanion), which is present in the mixture at the moment of introducing the initiator. The existence of region *2* is due, most likely, to a slow reversible equilibration of substance A with its inactive form D, which does not enter into the chemiluminescent reaction (Scheme 5).

Scheme 5

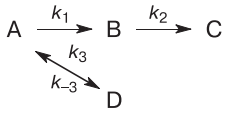

The kinetic dependence for region *1* (see Fig. 2) resembles the kinetic dependence of the chemiluminescent reaction of luminol. Its modeling was performed using the two-exponential approximation[21] by Eq. (1). The observed effective rate constants k_{1obs} and k_{2obs} were calculated by the iteration method.

$$I(t) = A[\exp(-k_{1obs}t) - \exp(-k_{2obs}t)] \quad (1)$$

The model curve obtained for region *1* (see Fig. 2) coincides well with the experimental kinetic dependence and, hence, the kinetic dependence for region *2* was determined by the subtraction of the experimental dependence from the overall experimental curve (*1* + *2*) (see Fig. 2). Since the measurements were carried out at the fixed temperature (25 °C), the found rate constants k_{1obs} and k_{2obs} are the same for each curve (see Fig. 1), and only the scaling factor *A*, which characterizes the concentration of substance A at the moment of chemiluminescent reaction onset C_A^0, changes.

$$A = C_A^0 \frac{k_{1obs}}{k_{1obs} + k_{2obs}} \quad (2)$$

The surface area under the model curve in region *1* (see Fig. 2) corresponds to the integrated intensity I_1 characterizing the amount of the active form of *N*-octylluminol (A) at the reaction onset. Figure 3 shows that longer intervals of time from the moment of reagent mixing (t_{mix}) correspond to lower I_1 values and lower the concentration C_A^0 directly related to I_1 by Eq. (2). Then I_1 reaches a plateau; *i.e.*, the kinetic dependence characteristic of reversible reactions is observed, and the equilibrium A ↔ D is strongly shifted toward form D. The observed rate constants k_{3obs} and k_{-3obs} were determined by the equation for reversible reactions[21]:

$$\ln\frac{y_e}{y_e - y} = (k_{3obs} + k_{-3obs})t, \quad (3)$$

where *y* is the conversion, and y_e is the equilibrium conversion. The model curve of the dependence of the inte-

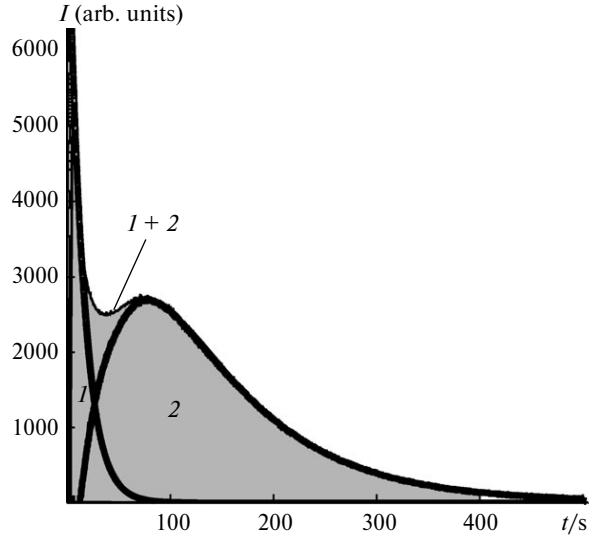

Fig. 2. Typical kinetic curve of the oxidation of *N*-octylluminol by the hypochlorite ion with area under the curve (*1* + *2*) divided into the regions corresponding to the consumption of the current amount of the *N*-octylluminol monoanion (*1*), which is present in the mixture at the moment of initiator introduction, and to the presence of a slow equilibration between the substance and its inactive form (*2*).

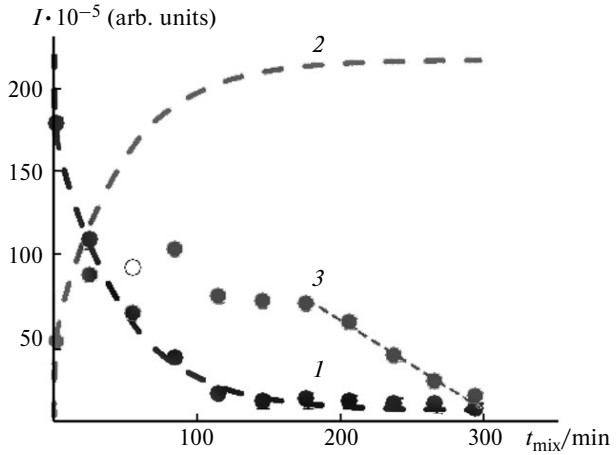

Fig. 3. Integrated intensity *I vs* time from the moment of mixing t_{mix}: calculated integrated intensities I_1 (*1*) and I_{2theor} (*2*) and the experimentally found integrated intensity I_2 (*3*).

grated intensity I_1 on time t_{mix} and the found values of the observed constants k_{3obs} and k_{-3obs} are well consistent with the experimental data (see Fig. 3).

The observed integrated intensity I_2 for region *2* (see Fig. 2) was determined subtracting I_1 from the overall integrated intensity I:

$$I_2 = I - I_1, \quad (4)$$

The material balance equation should be valid the substrate during the whole reaction:

$$C_{0,A}{}^0 = C_A{}^0 + C_D{}^0, \quad (5)$$

where $C_{0,A}{}^0$ is the concentration of *N*-octylluminol at the moment of mixing reagents ($t_{mix} = 0$), and $C_A{}^0$ and $C_D{}^0$ are the concentrations of two forms of the substrate directly at the moment of chemiluminescent reaction start. The expected integrated intensity I_{2theor} can be calculated using Eq. (5).

A comparison of the calculated I_{2theor} and experimentally found I_2 integrated intensities reveals an explicit divergence: the concentration of substance D does not reach a plateau and begins to decrease (see Fig. 3). At the same time, as mentioned earlier, the equilibrium concentration $C_A{}^0$ for substance A reaches a plateau, which inevitably indicates one more step of the process: transformation of form D into the "bound" form of *N*-octylluminol E that is not involved in the chemiluminescent reaction (Scheme 6).

Scheme 6

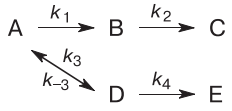

The dependence of the integrated intensity I on time t_{mix} can be divided into two parts: the first part corresponds to the first-order reaction and can be linearized in the logarithmic coordinates (Fig. 4, *b*), and the second part corresponds to the reaction of the zero order (see Fig. 4, *a*). The observed reaction order changes because of the replacement of the rate-determining step of the process. The equilibrium A ↔ D is established within the first ~120 min, further the decay kinetics of form D is observed in fact, and the observed rate constant k_{4obs} can be calculated by the equation for the zero-order reaction[21]:

$$C_A = C_A{}^0 - k_{4obs}t. \quad (6)$$

The modeled dependence of the *N*-octylluminol concentration on time t_{mix} coincides with the experimentally found dependence in the region of the established equilibrium A ↔ D (see Fig. 4, *a*).

The kinetic equations for this system take the following form:

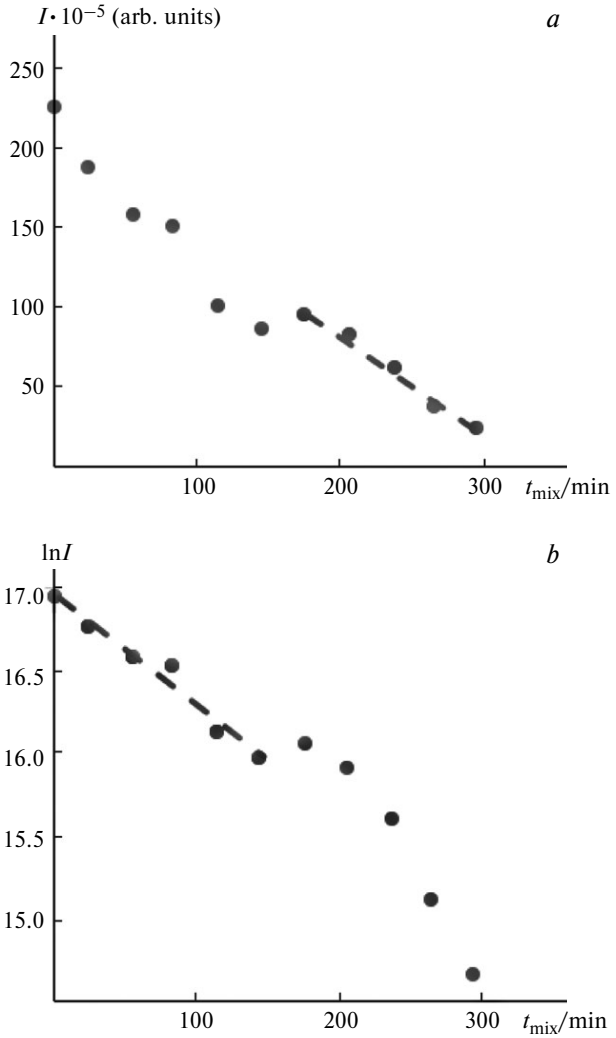

Fig. 4. Overall integrated intensity I *vs* time t_{mix} (*a*) and its logarithmic form (*b*).

$$\frac{dC_A}{d\tau} = -k_1[B] - k_3[D] + k_{-3}[D],$$
$$\frac{dC_B}{d\tau} = k_1[A] - k_2[C],$$
$$\frac{dC_C}{d\tau} = k_2[B],$$
$$\frac{dC_D}{d\tau} = k_3[A] - k_{-3}[A] - k_4[E],$$
$$\frac{dC_E}{d\tau} = k_4[D]. \quad (7)$$

The following apparent rate constants were obtained: $k_{1obs} = 5.62$ min^{-1}, $k_{2obs} = 135.43$ min^{-1}, $k_{3obs} = 2.09 \cdot 10^{-2}$ min^{-1}, $k_{-3obs} = 7.45 \cdot 10^{-4}$ min^{-1}, and $k_{4obs} = 3.14 \cdot 10^{-6}$ mol L^{-1} min^{-1}. A comparison in the logarithmic coordinates of the constants k_{1obs} and k_{2obs} with the constants found for the system based on luminol is presented in Fig. 5. It is seen that the variation of the concentrations of the substrate (C_{sub}), hypochlorite ion ($C(ClO^-)$), and hydroxide ions ($C(OH^-)$) is accompanied

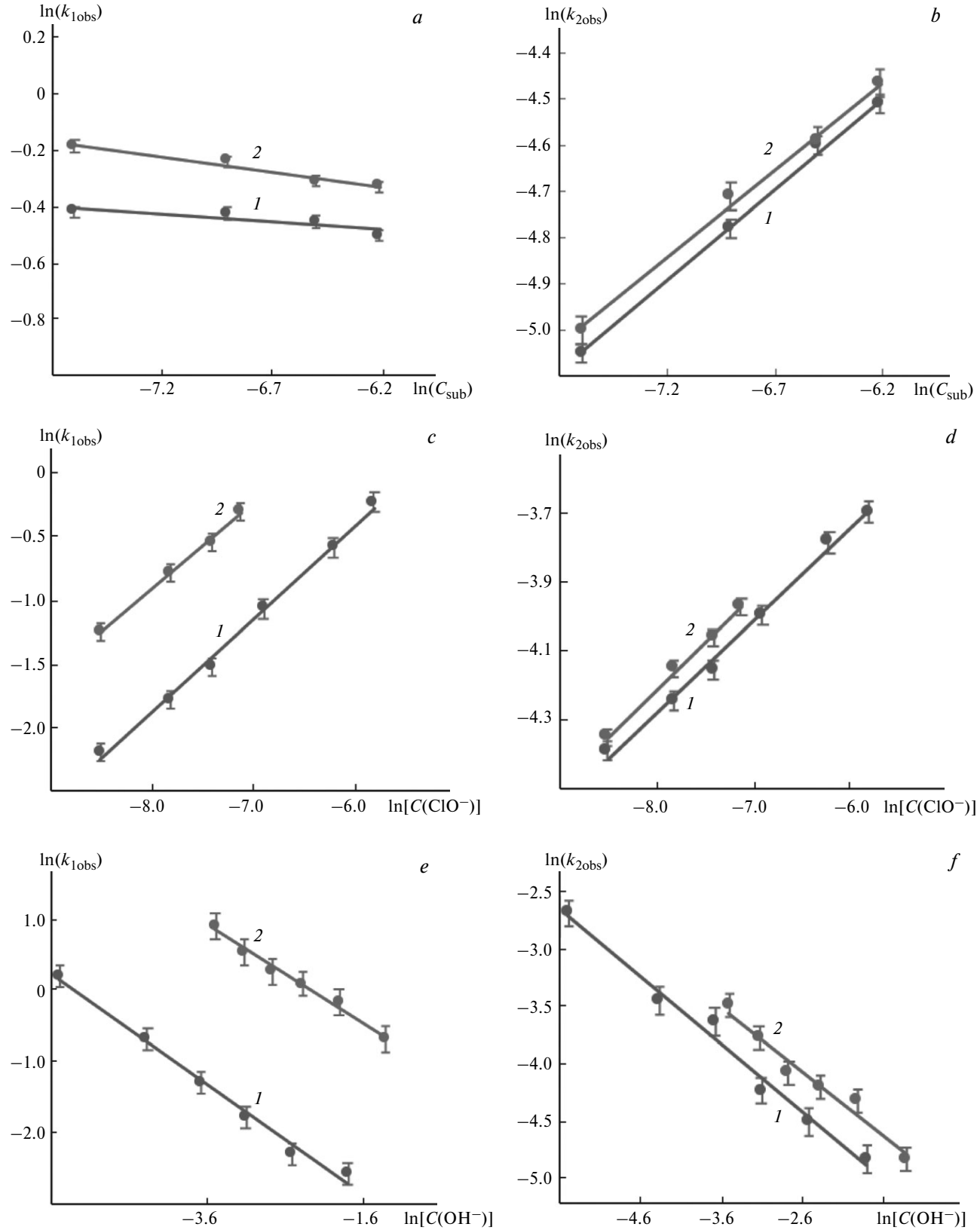

Fig. 5. Logarithmic dependence of the observed rate constants k_{1obs} (*a*, *c*, *e*) and k_{2obs} (*b*, *d*, *f*) on the concentrations of the substrate C_{sub} (*a*, *b*), hypochlorite ion $C(ClO^-)$ (*c*, *d*), and hydroxide ion $C(OH^-)$ (*e*, *f*) for the chemiluminescent oxidation of luminol (*1*) and *N*-octylluminol (*2*).

by a parallel change in the constants, and the angular coefficients of the dependences for the compared systems coincide. The latter indicates that the formal kinetic orders with respect to substances involved in the reaction coincide, which confirms the identity of the mechanisms leading to chemiluminescence in both systems. Note that the absolute values of k_{1obs} for *N*-octylluminol increase, since the corresponding dependences on all plots lie higher than the values obtained for luminol. This indicates an increase in the efficiency of the step of interaction of the luminogenous substrate with the initiator of the reaction. A nearly complete coincidence of k_{2obs} obtained for *N*-octylluminol with the values for the classical system based on luminol is observed. Evidently, the modification of the substrate exerted no effect on the step responsible for the transformation of intermediate product B into aminophthalic acid C in the excited state (see Scheme 3). It should be mentioned that the observed formal kinetic orders are half-integers (Table 1); *i.e.*, the steps of the considered scheme are presented by complex reactions. Nevertheless, their true rate constants of the step k_1 and k_2 can be calculated by the equation:

$$k_{obs} = kC_{sub}{}^{m}C_{ClO^-}{}^{n}C_{OH^-}{}^{p}, \quad (8)$$

where C_{sub} is the concentration of the substrate (*N*-octylluminol), C_{ClO^-} is the concentration of the hypochlorite ion, C_{OH^-} is the concentration of the hydroxide ion, m is the reaction order with respect to the substrate, n is the reaction order with respect to the hypochlorite ion, and p is the reaction order with respect to the hydroxide ion. The true rate constants of the first (k_1) and second (k_2) steps are 37.65 and $3.49 \cdot 10^4$ min^{-1}, respectively.

To conclude, we established the scheme and calculated the formal kinetic parameters for the chemiluminescent reaction of *N*-octylluminol with the hypochlorite ion. It is shown, that upon transfer to the selforganized micellar medium the efficiency of the step of the reaction of the luminogenous substrate with the initiator of the reaction increases significantly due to the effect of microconcentration. This results in an increase in the detected chemiluminescence intensities (maximum I_{max} and integrated I) by an order of magnitude. However, as compared to the mechanism determined for unmodified luminol, the scheme of the reaction in the system based on *N*-octylluminol is more complicated. In addition to the direct luminogeneous oxidation reaction, the mechanism of which coincides for both systems, *N*-octylluminol is reversibly transformed into the non-luminescent form, and the equilibrium is strongly shifted toward the latter. The reversible step results in the appearance of the second peak on the observed kinetic curve of the chemiluminescent reaction of *N*-octylluminol and a three fold decrease in the maximum intensity I_{max} within 5 h. The integrated intensity I decreases 11 times, indicating a slow transformation of the luminogeneous substrate into the inactive form. However, even under these conditions, the intensity of the observed analytical signal is 2.5 times that of the signal characteristic of the classical system.

Table 1. Formal kinetic parameters for the chemiluminescent oxidation of luminol and *N*-octylluminol by the hypochlorite ion

Substrate	*m*		*n*		*p*	
	k_1	k_2	k_1	k_2	k_1	k_2
Luminol	0	0.5	1	0.5	−0.5	−0.5
N-Octylluminol	0	0.5	1	0.5	−0.5	−0.5

Notes: m is the observed order with respect to the substrate, n is the order with respect to the hypochlorite ion, and p and the order with respect to the hydroxide ion.

Immediately after mixing maximum and integrated luminescence intensities of the luminescent system increase by an order of magnitude. It can be therefore inferred that the transition to systems with controlled mixing of the reagents, for example, flow—injection[12,13] or microfluid,[22] will make it possible to eliminate the observed drawbacks and attain the maximum efficiency of application of the newly synthesized luminogenous substrate.

This work was carried out in the framework of the state assignment of the Russian Federation (Theme No. 0706-2020-0020).

References

1. Ch. A. Marquette, L. J. Blum, *Anal. Bioanal. Chem.*, 2006, **385**, 546—554; DOI: 10.1007/s00216-006-0439-9.
2. M. Iranifam, *Luminescence*, 2013, **28**, № 23, 798—820; DOI: 10.1002/bio.2441.
3. G. Chen, M. Jin, P. Du, Ch. Zhang, X. Cui, Y. Zhang, J. Wang, F. Jin, Y. She, H. Shao, S. Wang, L. Zheng, *Food Agr. Immunol.*, 2017, **28**, 315—327; DOI: 10.1080/09540105.2016.1272550.
4. H. Zhu, Z. Jia, M. A. Trush, Y. R. Li, *React. Oxyg. Species*, 2016, **1**, 216—227; DOI: 10.20455/ros.2016.841.
5. J.-S. Kim, K. Jeong, J. M. Murphy, Y. A. R. Rodriguez, S.-T. S. Lim, *Oxid. Med. Cell. Longev.*, 2019, **2019**, 1754593; DOI: 10.1155/2019/1754593.
6. J. N. Miller, M. B. Nawawi, C. Burgess, *Anal. Chim. Acta*, 1992, **266**, 339—343; DOI: 10.1016/0003-2670(92)85061-A.
7. S. V. Khlyntseva, Ya. R. Bazel, A. B. Vishnikin, V. Andruch, *J. Anal. Chem.*, 2009, **64**, 657—673; DOI: 10.1134/S1061934809070028.
8. T. Kamidate, K. Yanashita, H. Tani, A. Ishida, M. Notani, *Anal. Chem.*, 2006, **78**, 337—342; DOI: 10.1021/ac058038n.
9. *Metody kontrolya. Biologicheskie i mikrobiologicheskie faktory. Ekspress-metod opredeleniya mikrobiologicheskikh pokazatelei kachestva pit´evoi vody, vody poverkhnostnykh vod i podzemnykh istochnikov. Metodicheskie ukazaniya* [*Monitoring Methods. Biological and Microbiological Factors. Express Method for Determination of Microbiological Indicators of Quality of Drinking Water, Surface Waters, and Underground Sources.*

Methodical Indications], Metodika, Ministry of Health Protection of RF, No. 1100/83-99-23 of 18.01.99 (in Russian).
10. Pat. RF 2276190, *Byul. Izobret.* [*Invention's Bulletin*], 2006, No. 13, 7 (in Russian).
11. N. A. Alarfaj, M. F. El-Tohamya, *Luminescence*, 2015, **30**, 3—11; DOI: 10.1002/bio.2694.
12. J. Cao, H. Wang, Y. Liu, *Spectrochim. Acta A*, 2015, **140**, 162—165; DOI: 10.1016/j.saa.2014.12.105.
13. D. Zhao, G. Zhang, T. Jiang, Zh. Deng, Y. Wu, *Intern. J. Environ. Anal. Chem.*, 2015, **95**, 980—988; DOI: 10.1080/03067319.2015.1077518.
14. J. Lasovsky, M. Rypka, J. Slouka, *J. Lumin.*, 1995, **65**, 25—32; DOI: 10.1016/0022-2313(95)00050-Z.
15. A. Karabchevsky, A. Mosayyebi, A. Kavokin, *Light Sci. Appl.*, 2016, **5**, e16164; DOI: 10.1038/lsa.2016.164.
16. T. V. Yan´kova, *Materialy Mezhdunarod. Molodezh. Nauch. Foruma* [*Proc. Intern. Youth Scientific Forum*] *"Lomonosov-2018" (Moscow, April 9—13, 2018)*, MGU, 2018, pp. 904—904 (in Russian).
17. T. V. Yankova, P. V. Melnikov, N. K. Zaytsev, *Moscow Univ. Chem. Bull.*, 2019, **74**, 116—121; DOI: 10.3103/S002713141903012X.
18. T. V. Yan´kova, P. V. Mel´nikov, N. A. Yashtulov, N. K. Zaitsev, *Tonkie Khim. Tekhnologii* [*Fine Chemical Technologies*], 2019, **14**, 90—97 (in Russian); DOI: 10.32362/2410-6593-2019-14-3-90-97.
19. M. Yamaguchi, H. Yoshida, H. Nohta, *J. Chromatogr. A*, 2002, **950**, 1—19; DOI: 10.1016/s0021-9673(02)00004-3.
20. R. F. Vasil´ev, *Sov. Phys. Usp.*, 1967, **9**, 504—524; DOI: 10.1070/PU1967v009n04ABEH003006.
21. B. V. Romanovskii, *Osnovy khimicheskoi kinetiki* [*Foundations of Chemical Kinetics*], Ekzamen, Moscow, 2006, 415 pp. (in Russian).
22. B. Hu, J. Li, L. Mou, Y. Liu, J. Deng, W. Qian, J. Sun, R. Cha, X. Jiang, *Lab. Chip.*, 2017, **17**, 2225—2234; DOI: 10.1039/C7LC00249A.

Received May 26, 2020;
in revised form June 22, 2020;
accepted August 20, 2020